



# Ppb-level NH<sub>3</sub> photoacoustic sensor combining a hammer-shaped tuning fork and a 9.55 μm quantum cascade laser

Shangzhi Li<sup>a,b,1</sup>, Yupeng Yuan<sup>b,1</sup>, Zhijin Shang<sup>c,d</sup>, Xukun Yin<sup>e</sup>, Angelo Sampaolo<sup>f</sup>,  
Pietro Patimisco<sup>f</sup>, Vincenzo Spagnolo<sup>c,f</sup>, Lei Dong<sup>c,d,\*</sup>, Hongpeng Wu<sup>c,d,\*</sup>

<sup>a</sup> Science and Technology on Analog Integrated Circuit Laboratory, Chongqing 401332, PR China

<sup>b</sup> CETC Chips Technology Group Co., LTD, Chongqing 401332, PR China

<sup>c</sup> State Key Laboratory of Quantum Optics and Quantum Optics Devices, Institute of Laser Spectroscopy, Shanxi University, Taiyuan 030006, PR China

<sup>d</sup> Collaborative Innovation Center of Extreme Optics, Shanxi University, Taiyuan 030006, PR China

<sup>e</sup> School of Optoelectronic Engineering, Xidian University, Xi'an 710071, PR China

<sup>f</sup> PolySense Lab-Dipartimento Interateneo di Fisica, University and Politecnico of Bari, Via Amendola 173, Bari, Italy

## ARTICLE INFO

### Keywords:

Quartz enhanced photoacoustic spectroscopy  
Atmospheric NH<sub>3</sub> detection  
Custom quartz tuning fork

## ABSTRACT

We present a quartz enhanced photoacoustic spectroscopy (QEPAS) gas sensor designed for precise monitoring of ammonia (NH<sub>3</sub>) at ppb-level concentrations. The sensor is based on a novel custom quartz tuning fork (QTF) with a mid-infrared quantum cascade laser emitting at 9.55 μm. The custom QTF with a hammer-shaped prong geometry which is also modified by surface grooves is designed as the acoustic transducer, providing a low resonance frequency of 9.5 kHz and a high-quality factor of 10263 at atmospheric pressure. In addition, a temperature of 50 °C and a large gas flow rate of 260 standard cubic centimeters per minute (scm) are applied to mitigate the adsorption and desorption effect arising from the polarized molecular of NH<sub>3</sub>. With 80-mW optical power and 300-ms lock-in integration time, the detection limit is achieved to be 2.2 ppb which is the best value reported in the literature so far for NH<sub>3</sub> QEPAS sensors, corresponding to a normalized noise equivalent absorption coefficient of  $1.4 \times 10^{-8} \text{ W cm}^{-1} \text{ Hz}^{-1/2}$ . A five-day continuous monitoring for atmospheric NH<sub>3</sub> is performed, verifying the stability and robustness of the presented QEPAS-based NH<sub>3</sub> sensor.

## 1. Introduction

Ammonia (NH<sub>3</sub>), a colorless, poisonous, alkaline gas with a strong pungent odor, constitutes the major component of total reactive nitrogen. The primary source of atmospheric NH<sub>3</sub> arises from agricultural emissions, which encompass animal husbandry and the application of NH<sub>3</sub>-based fertilizers. Additionally, NH<sub>3</sub> emission originates from diverse sources such as industrial processes, vehicular emissions and volatilization from soils and oceans [1–4]. Currently, ammonia represents one of the significant contributors to atmospheric pollution. This is primarily attributed to the reaction of NH<sub>3</sub> reacts with acidic gases in the atmosphere, resulting in the formation of ammonium salts that contribute to the generation of particulate matter (PM<sub>2.5</sub>) in the atmosphere. Despite its involvement in photochemical smog, acid rain and aerosol deposition, NH<sub>3</sub> is not regulated under the National Ambient Air

Quality Standards by the US Environmental Protection Agency (EPA), causing substantial difficulties and rigorous challenges to its emission reduction [5,6]. Therefore, sensitive and selective NH<sub>3</sub> detection has received considerable attention in the fields of environmental monitoring, chemical and pharmaceutical processing, and disease diagnosis.

To target these applications, various techniques have been developed and utilized for the detection of NH<sub>3</sub> concentration, including chemiluminescence, nanomaterials sensing and gas chromatography. However, these methods have limitations in selectivity and real-time monitoring, and easily introduce human errors which degrade the detection sensitivity and response time. Consequently, optical gas sensing techniques are being implemented frequently since the capabilities of fast response, high sensitivity and real-time monitoring [7–10]. For instance, tunable diode laser absorption spectrum (TDLAS), cavity ring down spectrum (CRDS), photo acoustic spectroscopy (PAS)

\* Corresponding authors at: State Key Laboratory of Quantum Optics and Quantum Optics Devices, Institute of Laser Spectroscopy, Shanxi University, Taiyuan 030006, PR China.

E-mail addresses: [donglei@sxu.edu.cn](mailto:donglei@sxu.edu.cn) (L. Dong), [wuhp@sxu.edu.cn](mailto:wuhp@sxu.edu.cn) (H. Wu).

<sup>1</sup> These authors contributed equally to this manuscript.

<https://doi.org/10.1016/j.pacs.2023.100557>

Received 31 July 2023; Received in revised form 29 August 2023; Accepted 11 September 2023

Available online 12 September 2023

2213-5979/© 2023 The Authors. Published by Elsevier GmbH. This is an open access article under the CC BY-NC-ND license (<http://creativecommons.org/licenses/by-nc-nd/4.0/>).

and difference optical absorption spectrum (DOAS) are typical ammonia detection methods based on laser absorption spectroscopy technology. Among these methods, PAS stands out as an appealing spectroscopic technique benefited from its simplicity, ruggedness and zero-background nature [11–13]. The PAS technique detects the photoacoustic signal generated from the selective absorption of modulated excitation energy and a wide-band microphone is employed as detecting element to collect the sound wave. In PAS-based sensors, the detection sensitivity depends on the geometry of the gas cell and the performance of microphone. Consequently, environmental noise can be easily introduced into the sensing system due to the low resonant frequency characteristics of the acoustic cell. Quartz enhanced photoacoustic spectroscopy (QEPAS), an alternative approach to PAS, utilizes a spectrophone consisting of a quartz tuning fork (QTF) and a resonant acoustic micro resonator (AmR) tube as an acoustic transducer to detect the weak sound wave [14–20]. This technique inherits PAS's inherent advantages of excitation-wavelength independence and sensitivity proportional to optical power. Compared to conventional PAS, the QTFs offer higher resonant frequencies ranging from several to tens of kHz and quality factors of  $\sim 10^4$ . In most of the QEPAS-based sensors, standard commercial QTFs with an oscillation frequency of 32.7 kHz and a frequency response bandwidth of nearly 3 Hz are exploited, enabling immunity to  $1/f$  ambient noise. Such characteristics make QEPAS one of the most attracted techniques for ambient  $\text{NH}_3$  detection. A. Kosterev et al. developed the QEPAS-based  $\text{NH}_3$  sensor utilizing a NIR laser source to detect  $\text{NH}_3$  and obtained a minimum detection limit (MDL) of 650 ppbv (parts per billion by volume) [21]. In 2015 and 2017, Wu et al. and Ma et al. combined QEPAS technique with erbium-doped fiber amplifier (EDFA) to detect  $\text{NH}_3$ , and the detection sensitivity ( $1\sigma$ ) of 1.6 ppmv and 481.4 ppbv, respectively, were achieved for an integration time of 1 sec [22,23]. However, the detection sensitivity is still insufficient to meet the requirements of atmospheric  $\text{NH}_3$  monitoring, and the utilization of EDFA complicated the QEPAS system and limited the ability of field application. In addition, several advanced QEPAS technologies have been developed to improve the detection sensitivity. In 2022, W. Ren et al. and H. Zeng et al. reported ultrasensitive doubly resonant QEPAS sensor and dual-comb QEPAS, respectively [24,25]. In 2023, W. Ren et al. developed a mid-infrared cavity-enhanced QEPAS sensor which is based on the doubly resonant photoacoustic effect, demonstrating highly sensitive photoacoustic excitation and high-resolution molecular spectroscopy. These methods also result in large systems and complex operations [26]. One possible solution is to select a mid-infrared laser which covers the stronger gas absorption lines as the excitation source for photoacoustic signals. Nevertheless, the 300- $\mu\text{m}$  prong spacing of this standard QTF can block a portion of laser beam. The laser light on the prongs leads to periodical heating of the QTF surface and result in a significant increase in background noise. This phenomenon is more pronounced for some excitation sources with degraded beam profile such as interband cascade laser (ICL), quantum cascade lasers (QCLs) and terahertz (THz) lasers, impeding the optical coupling between the QEPAS spectrophone and these advanced excitation source. Hence the design and investigation of QTFs' prong dimensions and geometry is requisite for the optimization of QEPAS-based sensing system.

In this work, we demonstrate a QEPAS-based gas sensor for ambient  $\text{NH}_3$  detection, in which a novel custom QTF with resonance frequency of 9538 Hz and a quality factor of 10263 at atmospheric pressure in air is employed as acoustic transducer. The custom QTF is designed with hammer-shaped surface-grooved prong geometry and a large prong spacing of 800  $\mu\text{m}$ , allowing the easier optical calibration operation compared with standard commercial QTF (300  $\mu\text{m}$ ). A QCL laser source emitting at 9.55  $\mu\text{m}$  is exploited in the system without spatial or laser modal beam filters which provides a higher detection sensitivity and a simpler system structure. The assessment of the proposed QEPAS-based sensor performance is implemented by a continuous atmospheric  $\text{NH}_3$  on-line monitoring, verifying the robustness and reliability of the sensor.

## 2. Sensor design and characterization

### 2.1. Selection of excitation wavelengths and optical sources

Since the fundamental vibrational of molecules is more than two orders stronger in the mid-infrared (MIR) spectral region than in the near infrared (NIR), a higher detection sensitivity can be obtained with a QEPAS sensor operated in MIR spectral region. According to the HITRAN database, four fundamental vibrational modes ( $\nu_1, \nu_2, \nu_3, \nu_4$ ) of the  $\text{NH}_3$  molecule are provided [27]. As demonstrated in Fig. 1,  $\text{NH}_3$  molecule has the strong  $\nu_2$  band and other hot band ( $2\nu_2-\nu_2$ ) near 10  $\mu\text{m}$  ( $1000 \text{ cm}^{-1}$ ) which is of great significance for trace  $\text{NH}_3$  detection in the infrared absorption spectra region due to the excellent line strengths compared with the other absorption bands. Taking into account the line strength and the absence of interference from other gas absorption, a  $\text{NH}_3$  absorption line located at  $1046.4 \text{ cm}^{-1}$ , with a line strength of  $3.648 \times 10^{-19} \text{ cm}^2/\text{mol}$ , was selected as the target line. This absorption line belongs to the  $\nu_2$  fundamental band of  $\text{NH}_3$  which is widely employed as a frequency standard for spectral calibration [28,29].

With the development of laser materials and the maturity of laser theory, the QCL laser has emerged as a highly versatile excitation source in the MIR spectral region for trace gas detection and environmental monitoring. In this study, a self-dependent compact QCL source (Healthyphoton, China, Model QC750-Touch™) with low current noise and temperature drift was selected for the sensing system. The QCL possess an integrated current and temperature control driver, and the temperature controller adopts non-PWM-type continuous current output control, greatly prolonging the service life of TEC devices. Additionally, a notable feature of the QCL is its maximum current soft clamping function, which prevents laser tube damage resulting from mishandling of high currents, ensuring the chip's safety to the utmost extent.

To target the  $\text{NH}_3$  absorption line, the QCL was coupled to a FTIR spectrometer (Thermo Scientific Model Nicolet iS50) to characterize the laser emitting wavelengths as shown in Fig. 2. The output wavelength can be tuned from  $1044.3 \text{ cm}^{-1}$  to  $1047.1 \text{ cm}^{-1}$ , covering the targeted line at  $1046.4 \text{ cm}^{-1}$  with a QCL temperature and current of 25.5  $^\circ\text{C}$  and 608 mA which was also depicted as a dotted line. The wavelength tuning coefficients of the QCL was calculated as  $-0.10496 \text{ cm}^{-1}/^\circ\text{C}$  and  $-0.00892 \text{ cm}^{-1}/\text{mA}$  by setting and changing the driving temperature and current, respectively.

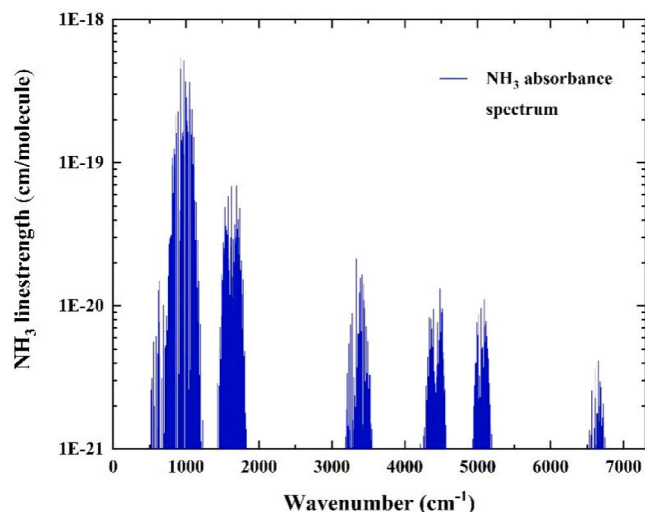


Fig. 1.  $\text{NH}_3$  absorbance spectra in the infrared region from 800 to 7000  $\text{cm}^{-1}$  according to the HITRAN database.

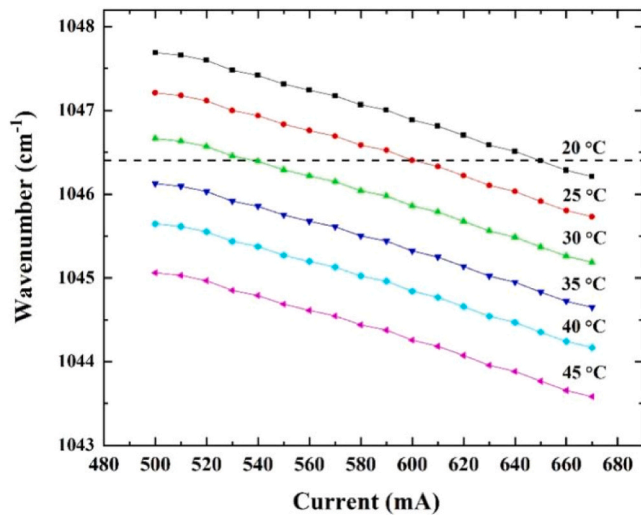


Fig. 2. The output wavelength of the QCL as a function of driving current from 500 mA to 670 mA at different temperature.

## 2.2. Design methodology of the hammer-shaped surface-grooved QTFs

For the photoacoustic detection of gases with adsorption characteristics, such as ammonia, mitigating the impact of gas adsorption on detection performance is crucial. One effective approach to achieve this is by minimizing the contact area of acoustoelectric transducers, such as QTF. Thus, it becomes essential to design the size and structure of the customized QTF carefully. The goal is to minimize its surface area while preserving its electrical parameters, including resonance frequency, quality factor, resistance value, and prong spacing, as well as charge collection efficiency. Consequently, the tuning fork can achieve optimal performance for ammonia detection. In this context, we present a novel tuning fork tailored specifically for atmospheric ammonia monitoring, meeting the aforementioned requirements. In principle, the QTF can be regarded as two vibratory prongs coupled with a supporting structure, and the prongs are joined at one base which are fixed to the supporting structure. When the laser beam is focused on the center of prongs to generate sound wave, the anti-symmetrical mode is dominant in the in-plane flexural vibration modes of QTF. To elastically describe the flexural mode vibration using a one-dimensional model, the free vibrating end of QTF prong can be specified by the following Euler-Bernoulli equation [30–32]:

$$EI \frac{\partial^4 y(x, t)}{\partial x^4} + \rho A \frac{\partial^4 y(x, t)}{\partial t^4} = 0 \quad (1)$$

where  $E = 0.72 \times 10^{11} \text{ N/m}^2$  and  $\rho = 2650 \text{ kg/m}^3$  are the elastic Young modulus and density of the quartz material, respectively.  $I$  and  $A$  represent the rotational inertia and the cross sectional area of the QTF prong,  $t$  is the time,  $x$  and  $y$  are the longitudinal and crossed directions relative to the prong. The fundamental resonance frequency can be solved and expressed by:

$$f = \frac{1.194^2 \pi w}{8\sqrt{12}l^2} \sqrt{\frac{E}{\rho}} \propto \frac{w}{l^2} \quad (2)$$

where  $w$ ,  $l$  are the prong width and length, respectively.

The ability of gas to efficiently relax the excess thermal energy dissipated through non-radiative relaxation process is dependent on the laser modulation frequency and the type of targeted gas. Hence it is crucial to ensure the condition  $\tau \ll 1/f$  is satisfied, enabling efficient gas excess energy relaxation. Here,  $\tau$  and  $1/f$  denote the molecular relaxation time and the laser modulation period, respectively [33–35]. Since the laser modulation frequency must match the oscillation

frequency  $f$  of the QTF in QEPAS sensor, the  $f$  of the custom QTF can be decreased with a reduced ratio of  $w$  and  $l$  to produce a maximum acoustic signal according to the Eq. (2) [36–38]. Additionally, the quality factor ( $Q$ -factor) related to the energy dissipation mechanisms of the QTF prong is also a major parameter for the sensor performance. Considering that the primary loss mechanism composed of surrounding fluid damping and support loss (which can be neglected in the fundamental mode) is strongly related to the geometric parameters of QTF prong, the  $Q$ -factor can be specified by [39–41]:

$$Q = \frac{Q_v}{1 + Q_v b P^c} \propto \frac{w l}{l} \quad (3)$$

where  $Q_v$  is the  $Q$ -factor of QTF in vacuum,  $P$  is the gas pressure,  $b$  and  $c$  are the special parameters relevant to the QTF dimensions and surrounding fluid viscosity, respectively.

To propose a novel QTF for the application of  $\text{NH}_3$  detection, two design requirements must be met: (1) reduce the resonance frequency  $f$  while maintaining a high  $Q$ -factor to guarantee the QEPAS response in  $\text{NH}_3$  gas; (2) increase the prong spacing to facilitate the optical alignment and improve the signal-to-noise ratio (SNR). In view of the V-T relaxation time of  $\text{NH}_3$  which is in the order of  $\sim 0.4 \mu\text{s}$ , the resonance frequency  $f$  of QTF is adopted as 9.5 kHz. Due to the sharp edge profiles of quartz crystal cannot be guaranteed with a chemical etching of  $t > 0.1 \text{ mm}$ , a thickness  $t$  is fixed at 0.25 mm. According to the equation (4) and (5), the ratio relationship between  $w$  and  $l$  needs to be considered and selected comprehensively to obtain a suitable  $f$  and  $Q$ -factor. To ensure the effective vibration of the QTF prongs, it is necessary to satisfy the condition  $t/w > 0.1$ . Therefore, a 2-mm width  $w$  and 9.4-mm prong length  $l$  was determined and used. An appropriate prong spacing is capable of providing excellent acousto-electric conversion efficiency, and reducing background noise when a MIR QCL is utilized. Hence a prong spacing of 800  $\mu\text{m}$  is chosen to match the spot size of the MIR excitation source.

The resonance frequency of QTF is determined by the crystal material and the geometry shape. When the prong size of the QTF is determined, the sensing property of the QTF can be further improved through a modification of prong geometry [40–43]. In this work, a

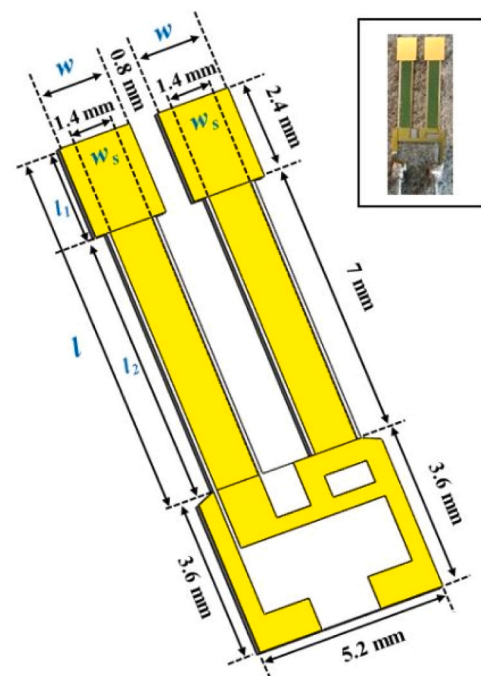


Fig. 3. Schematic of the geometrical dimensions of the hammer-shaped surface-grooved QTF. The inset shows the photograph of the novel QTF.

hammer-shaped QTF prong is designed and adopted, as shown in Fig. 3. This geometry provides an optimized stress field distribution, further enhancing the piezoelectric coupling efficiency. Moreover, based on the simulated result of COMSOL Multiphysics software in Ref 41, the intensity distribution of the stress field along the QTF prong reaches the maximum when  $w_s/w = 0.7$  mm. Although a lower frequency value can be achieved by reducing the ratio  $w_s/w$ , it may compromise the mechanical stability of the QTF due to the low moment of inertia [38]. Therefore,  $w_s$  is selected as 1.4 mm. Furthermore, a rectangular grooved modification with an area of  $1.8 \times 7$  mm and a depth of 0.05 mm is applied to each surface of QTF prong to improve the piezoelectric current and enhance piezoelectric effect without obvious negative effects on the Q-factor.

### 2.3. Experiment setup of QEPAS sensor system

A QEPAS sensor system based on a hammer-shaped surface-grooved QTF and a CW MIR QCL is demonstrated for  $\text{NH}_3$  detection. The experimental setup is schematically depicted in Fig. 4. The CW QCL (Healthyphoton, China, Model QC750-Touch™) emitting at  $9.55 \mu\text{m}$  is chosen as the excitation source to generate the QEPAS signals. An on-screen laser driver integrated with a cooling unit, a TEC temperature controller and a low noise current driver was employed to control the temperature and current of the QCL. The laser beam was focused into a  $\sim 0.25 \text{ mm}^2$  circular spot at the focal point by means of a 50-mm focal length plano-convex ZnSe lens, and can be directed easily through the dual tube spectrophone. The acoustic detection module (ADM) consists of the spectrophone configuration and two 25.4-mm diameter ZnSe windows with 98 % transmissivity efficiency, and has an internal volume of  $70 \text{ mm}^3$  capable of gas exchange. A power meter is placed behind the ADM to calibrate the beam and monitor the transmitted optical power.

In order to achieve sensitive  $\text{NH}_3$  detection, the  $2f$ -wavelength modulation spectroscopy (WMS) approach is employed. A dual-channel function generator is utilized to generate a  $f/2$  sinusoidal modulation signal and a ramp scanning signal, which are combined to dither the QCL wavelength with an electrical adder. Then the piezoelectric signal from the custom QTF is amplified by a trans-impedance preamplifier and demodulated by a lock-in amplifier (Stanford Research Systems, Model SR830) in the  $2f$  mode. The LIA time constant and slope filter are set to 300 ms and 12 dB/octave, respectively, corresponding to a bandwidth of 0.833 Hz. A personal computer (PC) is used to collect and analyze the QEPAS data via a LabVIEW routine.

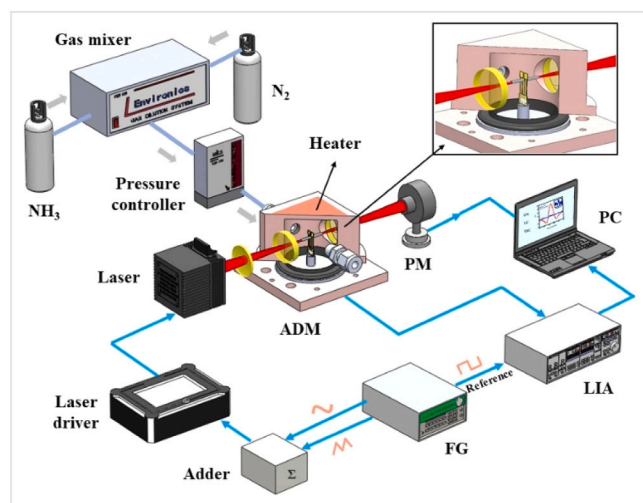


Fig. 4. Schematic of the developed QEPAS-based  $\text{NH}_3$  trace gas sensing system. ADM: acoustic detection module; PM: power meter; FG: function generator; LIA: lock-in amplifier.

A commercially available gas dilution system (Environics Inc. Model EN4040) is utilized to generate a mixture of  $\text{NH}_3/\text{N}_2$  gas at desired concentrations. To regulate the gas flow rate to the set point, a mass flow meter combined with a needle valve (Not shown in the figure) is placed downstream. The pressure inside the ADM is controlled and maintained at 700 torr via a pressure controller (MKS Instruments Inc. Model 649B13TS1M22 M) and a vacuum pump. A Nafion humidifier was inserted inline to keep the water concentration entering the QEPAS cell at 1.5 % to eliminate the influence of environmental water vapor changes on the experimental system. Nevertheless, the  $\text{NH}_3$  molecule is readily adsorbed to surfaces resulted from its viscosity and interaction with the ADM surface, preventing the accurate determination of the  $\text{NH}_3$  concentration in the QEPAS system. To mitigate this issue, a heater is tightly attached to the walls of the ADM. The purpose of the heater is to eliminate the adsorption and desorption effects arising from the polarized molecular of  $\text{NH}_3$ . This is due to the fact that a rise of temperature increases the thermal motion of  $\text{NH}_3$  gas molecules, increasing the gas desorption rate and reducing the total adsorption of gas. Experimental results show that with the increase of temperature, the response time of the system will be significantly shortened. Compared to the room temperature, the operating temperature of  $50^\circ\text{C}$  can reduce the response time by 65 %. Continuing to increase the temperature may further inhibit the adsorption of  $\text{NH}_3$ , but the high temperature puts forward new requirements for the heat resistance of the device and requires the addition of insulation devices. Hence, we finally set the operating temperature of the system at  $50^\circ\text{C}$ . In addition, a large gas flow rate of 260 sccm is adopted to reduce the  $\text{NH}_3$  molecular adsorbability and accelerate the gas exchange times.

## 3. Optimization and assessment of sensor performance

### 3.1. Parameter optimization

In order to improve the detection performance, it is necessary to optimize the parameters of the spectrophone configuration. Since the laser beam must be focused at the center of the prong spacing to vibrate the QTF prongs effectively, the focusing position of the laser beam has been investigated and determined as shown in Fig. 5(a). The QTF symmetry axis is vertically scanned by the laser beam from the top to bottom for acquiring the optimum focused spot position. The QEPAS signals are normalized to the maximum value and the optimum laser focus position is determined as 2 mm from the prong top which is depicted in Fig. 5(b). In this work, a 50-ppm  $\text{NH}_3/\text{N}_2$  mixture was selected as target gas.

In most QEPAS-based trace gas sensors, an on-beam spectrophone configuration is commonly employed to achieve a higher signal-noise-ratio (SNR) gain [44–46]. In this configuration, the AmR consists of two identical metallic tubes positioned symmetrically and aligned perpendicular to the QTF plane, with the QTF inserted at the center. To enhance the acoustic coupling efficiency, the dimension parameters

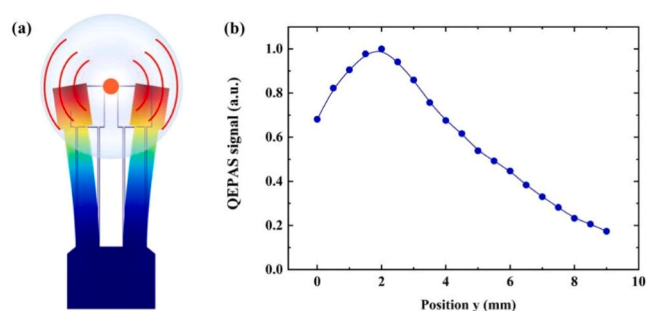


Fig. 5. (a) Diagram of the QTF prongs deformation vibrating in the fundamental flexural mode via COMSOL MultiPhysics. The spot position represents the starting point of scanning. (b) Normalized QEPAS signals as a function of the position along the vertical symmetry axis of the QTF.

(inner diameter and tube length) are tested and optimized at atmospheric pressure. Since the inner diameter (ID)  $d$  is related with the prong spacing, eight different AmRs with  $d = 1$  mm, 1.25 mm, 1.35 mm, 1.5 mm, 1.65 mm, 1.75 mm, 1.85 mm and 2.05 mm but with the same length  $l = 12$  mm have been tested. According to the related theoretical and experimental investigation, the length of each tube  $l$  is associated with the acoustic wavelength  $\lambda$  at the resonance frequency  $f$  of the QTF under the assumption that the QTF-tube distance is zero. However, with the insertion of QTF distorting the acoustic resonance in the AmR, the optimum AMR length ( $2l$ ) is  $\lambda/2 < 2l < \lambda$ , resulting in the optimal  $l$  of each tube between  $\lambda/4$  and  $\lambda/2$ . In this work, the acoustic wavelength  $\lambda$  for the custom 9.5-kHz QTF is 35.6 mm, hence a series of tubes with different lengths ( $8.9$  mm  $< l < 17.8$  mm) were measured. Fig. 6 demonstrates the optimum geometric parameters of the AmRs is  $d = 1.75$  mm and  $l = 13$  mm with a QTF-tube distance of  $200$   $\mu\text{m}$ , which provides a SNR gain factor of 37.

Generally, the photoacoustic signal in QEPAS-based sensors can be described by:  $S = CP_0\alpha(p)\epsilon(p)Q(p)$ , where  $C$  is the system constant,  $P_0$  is the optical power,  $p$  is the gas pressure,  $\alpha$ ,  $\epsilon$ ,  $Q$ , is the peak intensity of the  $2f$  absorption spectrum, optoacoustic transduction efficiency and QTF Q-factor, respectively. Since the  $\alpha$  depends on the modulation depth of the laser current, the laser modulation depth must match the  $p$ -dependent absorption linewidth. As depicted in Fig. 7, the modulation voltages in the ADM are measured and optimized under different gas pressures to achieve the maximum QEPAS signal using a 1-ppm  $\text{NH}_3/\text{N}_2$  calibration gas. The highest  $2f$  signal is observed at 300 torr with a modulation voltage of 180 mV, which is 40 % higher than the QEPAS signal obtained at 700-torr with a 300-mV voltage modulation depth.

For the  $\text{NH}_3$  detection sensing system, a large gas flow rate can retard the adsorption-desorption effect and reduce the gas exchange time in the ADM, but may cause an increase in the noise level [47]. Therefore, the dependence of the  $1\sigma$  noise level on different gas flow rate from 20 sccm to 400 sccm is demonstrated with the optimum AmR parameters as shown in Fig. 8. An obvious increase of noise is observed when the gas flow rate up to 280 sccm, which can be attributed to unwanted prong vibration. Hence a flow rate of 260 sccm is selected for the sensor operation.

Based on the measured noise level, a MDL of 1.3 ppb at 300 torr and 2.2 ppb at 700 torr is obtained at 80-mW optical power. The following works are implemented under the atmospheric pressure of 700 torr since the pressure controller can be removed, simplifying the sensing system. Consequently, a normalized noise equivalent absorption (NNEA) coefficient for  $\text{NH}_3$  of  $1.4 \times 10^{-8} \text{ W cm}^{-1}/\sqrt{\text{Hz}}$  is obtained at 700 torr.

### 3.2. Performance characteristics

To assess the performance of the QEPAS-based  $\text{NH}_3$  sensor, the system was operated with the optimum parameters under atmospheric pressure. Various concentration levels of  $\text{NH}_3$  from 100 ppb to 10 ppm

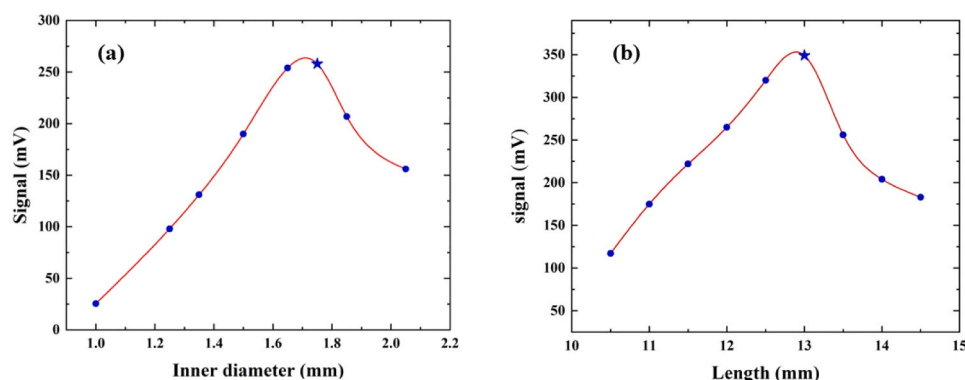


Fig. 6. QEPAS peak signals obtained with different (a) inner diameter and (b) length of each tube.

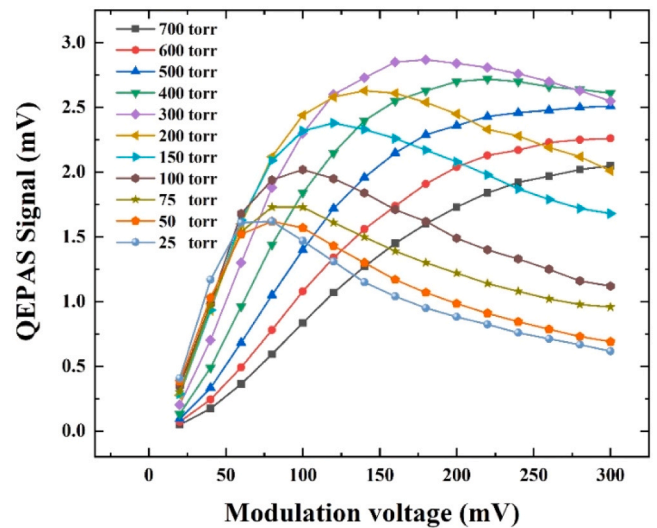


Fig. 7.  $2f$  QEPAS peak signal of  $\text{NH}_3$  spectra measured at different gas pressures and laser voltage modulation depths. All measurements were operated using a 1-ppm  $\text{NH}_3$  mixture in  $\text{N}_2$ .

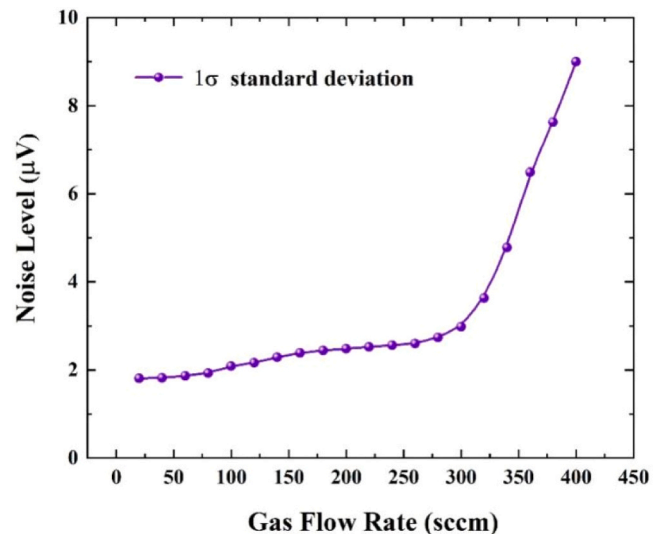


Fig. 8. Dependence of the noise level measured for pure  $\text{N}_2$  as a function of the gas flow rate in the range of 20–400 sccm at atmospheric pressure.

generated by the gas dilution system are filled into the ADM for characterizing the linearity of this sensor response to the  $\text{NH}_3$  concentration. For each concentration, more than 200 QEPAS signals are measured with an acquisition time of 1 s to determine the average value as the final signal value. From Fig. 9, an excellent linear response of the QEPAS peak signals and the  $\text{NH}_3$  concentration is indicated and confirmed.

The performance of the QEPAS-based sensor is further evaluated in terms of limits of detection of  $\text{NH}_3$  trace gas through Allan variance analysis which is a measurement index of system stability by quantifying noise. As shown in Fig. 10, the long-term stability and the sensitivity of the system are demonstrated with a 1-s acquisition time when the ADM is filled with pure  $\text{N}_2$  at atmospheric pressure. In addition, the wavelength of the QCL laser was locked at  $1046.4 \text{ cm}^{-1}$ , corresponding to the  $\text{NH}_3$  absorption peak. The deviation curve almost follows a  $1/\sqrt{t}$  dependence for time sequences ranging from 1 s to 52 s, revealing a white noise behavior, where  $t$  is the lock-in integration time. And the Allan-werle deviation experiences a sensitivity drift following a  $\sqrt{t}$  dependence when the averaging time exceeds 80 s. The calibration curve of the QEPAS sensor is used to convert the  $1\sigma$ -noise voltages into  $\text{NH}_3$  concentrations. Based on the Allan derivation curves, the MDL can be further lowered to 90 ppt with an averaging time of 52 s

In order to verify the sensor performance in practical application, a continuous monitoring of atmospheric  $\text{NH}_3$  concentration was implemented from September 7th to 11th, 2022, inside a laboratory located in the Shaw Amenities Building on the Shanxi University campus in Taiyuan, China. To collect atmospheric air samples, an external diaphragm pump was utilized to draw air from the outdoors. A  $3 \mu\text{m}$  micropore PTFE membrane was incorporated to prevent any potential adverse effects caused by dust or soot particles. The results of real-time continuous monitoring of atmospheric  $\text{NH}_3$  with an acquisition time of 1 s and at atmospheric pressure are depicted in Fig. 11. A periodic trend in  $\text{NH}_3$  concentration is observed from the measured results. Among them, the measured  $\text{NH}_3$  concentration has a morning spike around 07:00–10:00 each day, and decreased until reaching the minimum at 17:00. The diurnal variations of urban  $\text{NH}_3$  can be attributed to nonagricultural sources caused by human activities, meteorology, and chemical reactions, particularly the vehicular emissions [48]. For example, on colder mornings, more  $\text{NH}_3$  is produced in vehicle exhaust due to the higher frequency of fuel-rich combustion, favoring reduction processes on the catalyst surface, hence promotes the significant conversion of  $\text{NO}_x$  to  $\text{NH}_3$  rather than  $\text{N}_2$ . In addition, the low  $\text{NH}_3$  concentration may be due to the relatively high mixing layer height in the afternoon, resulting in a better mixing of  $\text{NH}_3$  and air. And the meteorological conditions after 16:00 are more conducive to the reaction of

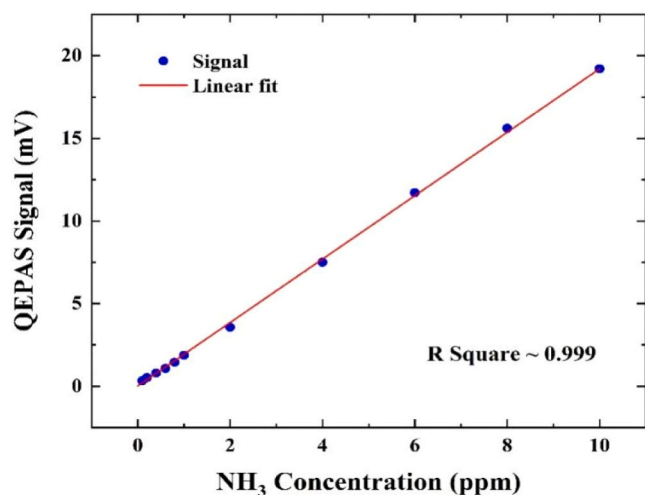


Fig. 9. The linear relationship between  $2f$  signal amplitude and  $\text{NH}_3$  concentration.

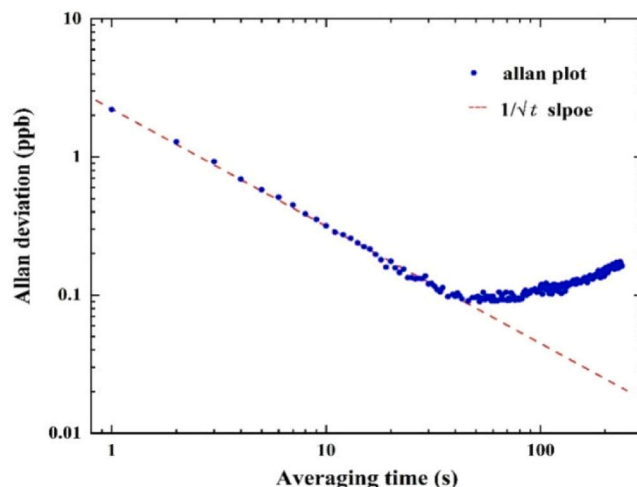


Fig. 10. Allan-werle deviation as a function of the averaging time.

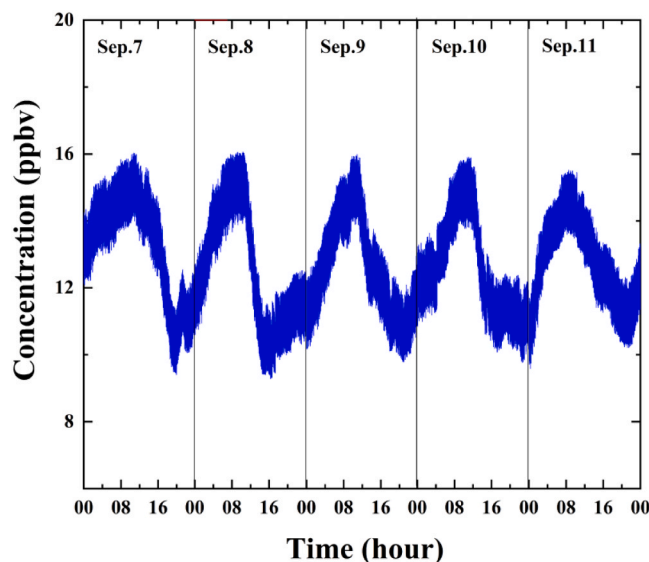


Fig. 11. Continuous five-day monitoring of environmental  $\text{NH}_3$  concentrations by the proposed sensor system.

$\text{NH}_3$  with acidic precursors and enhance the isotope exchange between  $\text{NH}_3$  and aerosol  $\text{NH}_4^+$ .

#### 4. Conclusion

A robust, compact and highly sensitive prototype of a QEPAS-based sensor for  $\text{NH}_3$  real-time monitoring is realized and demonstrated by combining a novel QTF with a mid-infrared QCL. The QTF, modified with a hammer-shaped prong geometry and surface grooves, is first customized for  $\text{NH}_3$  detection which results in a high-quality factor of 10263 at atmospheric pressure in air. The reduced QTF resonance frequency of 9.5 kHz perfectly matches the vibration-translation relaxation of  $\text{NH}_3$ , providing a more sensitive sensing performance. In addition, the 0.8-mm prong spacing permits the QEPAS operation with a MIR QCL which can pass easily through the ADM without spatial filters. The linear response of the  $\text{NH}_3$  sensor was exhibited and a minimum detection limit of 2.2 ppb with 300-ms integration time is obtained, corresponding to a NNEA of  $1.4 \times 10^{-8} \text{ W cm}^{-1} \text{ Hz}^{-1/2}$ , which is the best value reported so far for  $\text{NH}_3$  QEPAS sensors. Continuous monitoring of atmospheric  $\text{NH}_3$  for five days was demonstrated, validating the performance the QEPAS-based  $\text{NH}_3$  sensing system. As part of future work, a design incorporating

a 3D-printed Teflon-based Acoustic Detection Module (ADM) will be developed to eliminate the adsorption–desorption effect of NH<sub>3</sub>. Furthermore, the system holds promise for non-invasive breath analysis diagnostics and ammonia monitoring in agriculture and animal husbandry, which are potential areas for its application.

### Declaration of Competing Interest

The authors declare that there are no conflicts of interest.

### Data Availability

Data will be made available on request.

### Acknowledgments

This work is supported by the Chongqing Postdoctoral Science Foundation (No. CSTB2023NSCQ-BHX0085); National Natural Science Foundation of China (Nos. 62122045, 62075119, 61622503, 62105252); Fundamental Research Funds for the Central Universities (No. QTZX23023); THORLABS GmbH, within PolySense, a joint-research laboratory; and Outstanding Innovative Teams of Higher Learning Institutions of Shanxi; Shanxi “1331 Project” key subject construction.

### References

- V.P. Aneja, P.A. Roelle, G.C. Murray, J. Southerland, J.W. Erisman, D. Fowler, W.A. H. Asman, N. Patni, Atmospheric nitrogen compound II: emissions, transport, transformation, deposition and assessment, *Atmos. Environ.* 35 (11) (2000) 1903–1911.
- L. Lamard, D.B. Harder, A. Peremans, J.C. Petersen, M. Lassen, Versatile photoacoustic spectrometer based on a mid-infrared pulsed optical parametric oscillator, *Atmos. Chem. Phys.* 11 (18) (2011) 9721–9733.
- Iowa State University and the University of Iowa Study Group: Iowa Concentrated Animal Feeding Operations Air Quality Study, Final Report (2002).
- E. Rafatmah, B. Hemmateenejad, Fabrication of the first disposable three-dimensional paper-based concentration cell as ammonia sensor with a new method for paper hydrophobization by Laser Patterned Parafilm®, *Electroanalysis* 31 (4) (2019) 632–638.
- K. Duan, M. Hu, Y. Ji, Z. Lu, S. Yao, W. Ren, High-temperature ammonia detection using heterodyne phase-sensitive dispersion spectroscopy at 9.06  $\mu\text{m}$ , *Fuel* 325 (2022), 124852.
- J.H. Seinfeld, S.N. Pandis, *Atmospheric Chemistry and Physics: From Air Pollution to Climate Change*, Wiley, New York, 1997.
- K. Zheng, C. Zheng, L. Hu, F. Song, Y. Zhang, Y. Wang, F.K. Tittel, Near-infrared fiber-coupled off-axis cavity-enhanced thermoelastic spectroscopic sensor system for in situ multipoint ammonia leak monitoring, *IEEE T. Instrum. Meas.* 70 (2021) 1–9.
- M.E. Webber, D.S. Baer, R.K. Hanson, Ammonia monitoring near 1.5  $\mu\text{m}$  with diode-laser absorption sensors, *Appl. Opt.* 40 (12) (2001) 2031–2042.
- H. Lu, C. Zheng, L. Zhang, Z. Liu, F. Song, X. Li, Y. Zhang, Y. Wang, A remote sensor system based on TDLAS technique for ammonia leakage monitoring, *sensors* 21 (7) (2021) 2448.
- Y. Ji, K. Duan, Z. Lu, W. Ren, Mid-infrared absorption spectroscopic sensor for simultaneous and in-situ measurements of ammonia, water and temperature, *Sens. Actuators B* 371 (2022), 132574.
- B. Rumburg, G.H. Mount, D. Yonge, B. Lamb, H. Westberg, M. Neger, J. Filipy, R. Kincaid, K. Johnson, Measurements and modeling of atmospheric flux of ammonia from an anaerobic dairy waste lagoon, *Atmos. Environ.* 42 (14) (2008) 3380–3393.
- J. Kong, N.R. Franklin, C. Zhou, M.G. Chapline, S. Peng, K. Cho, H. Dai, Nanotube molecular wires as chemical sensors, *Science* 87 (5453) (2000) 622–625.
- J.P. Besson, S. Schilt, L. Thévenaz, Sub-ppm multi-gas photoacoustic sensor, *Spectrochim. Acta A* 63 (5) (2006) 899–904.
- A.A. Kosterev, Y.A. Bakhrin, R.F. Curl, F.K. Tittel, Quartz-enhanced photoacoustic spectroscopy, *Opt. Lett.* 27 (21) (2002) 1902–1904.
- A.A. Kosterev, F.K. Tittel, D.V. Serebryakov, A.L. Malinovsky, I.V. Morozov, Applications of quartz tuning forks in spectroscopic gas sensing, *Rev. Sci. Instrum.* 76 (4) (2005), 043105.
- K. Chen, H. Deng, M. Guo, C. Luo, S. Liu, B. Zhang, F. Ma, F. Zhu, Z. Gong, W. Peng, Q. Yu, Tube-cantilever double resonance enhanced fiber-optic photoacoustic spectrometer, *Opt. Laser Technol.* 123 (2020), 105894.
- L. Hu, C. Zheng, M. Zhang, D. Yao, J. Zheng, Y. Zhang, Y. Wang, F.K. Tittel, Quartz-enhanced photoacoustic spectroscopic methane sensor system using a quartz tuning fork-embedded, double-pass and off-beam configuration, *Photoacoustics* 18 (2020), 100174.
- P. Patimisco, A. Sampaolo, L. Dong, F.K. Tittel, V. Spagnolo, Recent advances in quartz enhanced photoacoustic sensing, *Appl. Phys. Rev.* 5 (1) (2018), 011106.
- K. Liu, X. Guo, H. Yi, W. Chen, W. Zhang, X. Gao, Off-beam quartz-enhanced photoacoustic spectroscopy, *Opt. Lett.* 34 (10) (2009) 1594–1596.
- Z. Wang, M. Yang, L. Fu, C. Chen, R. You, W. Ren, Rapid field measurement of ventilation rate using a quartz-enhanced photoacoustic SF<sub>6</sub> gas sensor, *Meas. Sci. Technol.* 31 (8) (2020), 085105.
- A.A. Kosterev, F.K. Tittel, Ammonia detection by use of quartz-enhanced photoacoustic spectroscopy with a near-IR telecommunication diode laser, *Appl. Opt.* 43 (33) (2004) 6213–6217.
- H. Wu, L. Dong, X. Liu, H. Zheng, X. Yin, W. Ma, L. Zhang, W. Yin, S. Jia, Fiber-amplifier-enhanced QEPAS sensor for simultaneous trace gas detection of NH<sub>3</sub> and H<sub>2</sub>S, *Sensors* 15 (10) (2015) 26743–26755.
- Y. Ma, Y. He, Y. Tong, X. Yu, F.K. Tittel, Ppb-level detection of ammonia based on QEPAS using a power amplified laser and a low resonance frequency quartz tuning fork, *Opt. Express* 25 (23) (2017) 29356–29364.
- Z. Wang, Q. Wang, H. Zhang, S. Borri, I. Galli, A. Sampaolo, P. Patimisco, V. Spagnolo, P. Natale, W. Ren, Doubly resonant sub-ppt photoacoustic gas detection with eight decades dynamic range, *Photoacoustics* 27 (2022), 100387.
- X. Ren, M. Yan, Z. Wen, H. Ma, R. Li, K. Huang, H. Zeng, Dual-comb quartz-enhanced photoacoustic spectroscopy, *Photoacoustics* 28 (2022), 100403.
- Q. Nie, Z. Wang, S. Borri, P.D. Natale, W. Ren, Mid-infrared swept cavity-enhanced photoacoustic spectroscopy using a quartz tuning fork, *Appl. Phys. Lett.* 123 (5) (2023), 054102.
- The HITRAN Database. Available online: (<http://www.hitran.com>).
- V.A. Job, N.D. Patel, R.D. Cunha, V.B. Kartha, High resolution diode laser measurements on the  $\nu_2$  bands of <sup>14</sup>NH<sub>3</sub> and <sup>15</sup>NH<sub>3</sub>, *J. Mol. Spectrosc.* 101 (1) (1983) 48–60.
- F. Cappellani, G. Restelli, Diode laser measurements of NH<sub>3</sub>  $\nu_2$ -band spectral lines, *J. Mol. Spectrosc.* 77 (1) (1979) 36–41.
- P. Patimisco, S. Borri, A. Sampaolo, H.E. Beere, D.A. Ritchie, M.S. Vitiello, G. Scarmario, V. Spagnolo, A quartz enhanced photo-acoustic gas sensor based on a custom tuning fork and a terahertz quantum cascade laser, *Analyst* 139 (9) (2014) 2079–2087.
- A. Sampaolo, P. Patimisco, R. Pennetta, G. Scarmario, F.K. Tittel, V. Spagnolo, New approaches in quartz-enhanced photoacoustic sensing, *Proc. SPIE* 9370 (2015) 93700X.
- P. Patimisco, A. Sampaolo, L. Dong, M. Giglio, G. Scarmario, F.K. Tittel, V. Spagnolo, Analysis of the electro-elastic properties of custom quartz tuning forks for photoacoustic gas sensing, *Sens. Actuators B* 227 (2016) 539–546.
- H. Wu, L. Dong, X. Yin, A. Sampaolo, P. Patimisco, W. Ma, L. Zhang, W. Yin, L. Xiao, V. Spagnolo, S. Jia, Atmospheric CH<sub>4</sub> measurement near a landfill using an ICL-based QEPAS sensor with VT relaxation self-calibration, *Sens. Actuators B* 297 (2019), 126753.
- C. Gaudio, A. Volpe, A. Ancona, One-step femtosecond laser stealth dicing of quartz, *Micromachines* 11 (3) (2020) 327.
- A.A. Kosterev, Y.A. Bakhrin, F.K. Tittel, Ultrasensitive gas detection by quartz-enhanced photoacoustic spectroscopy in the fundamental molecular absorption bands region, *Appl. Phys. B* 80 (1) (2005) 133–138.
- P. Patimisco, A. Sampaolo, H. Zheng, L. Dong, F.K. Tittel, V. Spagnolo, Quartz-enhanced photoacoustic spectrophones exploiting custom tuning forks: a review, *Adv. Phys. X* 2 (1) (2017) 169–187.
- H. Wu, A. Sampaolo, L. Dong, P. Patimisco, X. Liu, H. Zheng, X. Yin, W. Ma, L. Zhang, W. Yin, V. Spagnolo, S. Jia, F.K. Tittel, Quartz enhanced photoacoustic H<sub>2</sub>S gas sensor based on a fiber-amplifier source and a custom tuning fork with large prong spacing, *Appl. Phys. Lett.* 107 (11) (2015), 111104.
- B. Sun, A. Zifarelli, H. Wu, S.D. Russo, S. Li, P. Patimisco, L. Dong, V. Spagnolo, Mid-infrared quartz-enhanced photoacoustic sensor for ppb-level CO detection in a SF<sub>6</sub> gas matrix exploiting a T-grooved quartz tuning fork, *Anal. Chem.* 92 (20) (2020) 13922–13929.
- Z. Hao, A. Erbil, F. Ayazi, An analytical model for support loss in micromachined beam resonators with in-plane flexural vibrations, *Sens. Actuat. A-Phys.* 109 (1–2) (2003) 156–164.
- H. Hosaka, K. Itao, S. Kuroda, Damping characteristics of beam-shaped micro-oscillators, *Sens. Actuat. A-Phys.* 49 (1–2) (1995) 87–95.
- P. Patimisco, A. Sampaolo, M. Giglio, S.D. Russo, V. Mackowiak, H. Rossmadl, A. Cable, F.K. Tittel, V. Spagnolo, Tuning forks with optimized geometries for quartz-enhanced photoacoustic spectroscopy, *Opt. Express* 27 (2) (2019) 1401–1415.
- P. Patimisco, G. Scarmario, F.K. Tittel, V. Spagnolo, Quartz-enhanced photoacoustic spectroscopy: a review, *Sensors* 14 (4) (2014) 6165–6206.
- S. Li, L. Dong, H. Wu, A. Sampaolo, P. Patimisco, V. Spagnolo, F.K. Tittel, Ppb-level quartz-enhanced photoacoustic detection of carbon monoxide exploiting a surface grooved tuning fork, *Anal. Chem.* 91 (9) (2019) 5834–5840.
- L. Dong, A.A. Kosterev, D. Thomazy, F.K. Tittel, QEPAS spectrophones: design, optimization, and performance, *Appl. Phys. B: Lasers Opt.* 100 (3) (2010) 627–635.
- M. Mordmüller, M. Köhring, W. Schade, U. Willer, *Appl. Phys. B: Lasers Opt.* 119 (1) (2015) 111–118.

- [46] H. Zheng, L. Dong, X. Yin, H. Wu, L. Zhang, W. Ma, W. Yin, S. Jia, X. Liu, Ppb-level QEPAS NO<sub>2</sub> sensor by use of electrical modulation cancellation method with a high power blue LED, *Sens. Actuators, B* 208 (2015) 173–179.
- [47] X. Yin, H. Wu, L. Dong, B. Li, W. Ma, L. Zhang, W. Yin, L. Xiao, S. Jia, F.K. Tittel, Ppb-Level SO<sub>2</sub> photoacoustic sensors with a suppressed absorption–desorption effect by using a 7.41 μm external-cavity quantum cascade laser, *ACS Sens* 5 (2) (2020) 549–556.
- [48] M. Gu, Y. Pan, W.W. Walters, Q. Sun, L. Song, Y. Wang, Y. Xue, Y. Fang, Vehicular emissions enhanced ammonia concentrations in winter mornings: insights from diurnal nitrogen isotopic signatures, *Environ. Sci. Technol.* 56 (2022) 1578–1585.



**Shangzhi Li** received his Ph.D. degree in atomic and molecular physics in the Institute of Laser Spectroscopy of Shanxi University, China, in 2022. Currently he is an engineer in CETC Chips Technology Group Co., LTD, Chongqing, China. His research interests include gas sensor, photoacoustic spectroscopy and laser spectroscopy techniques.



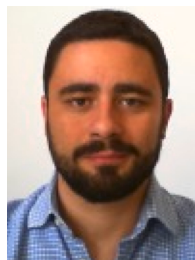
**Yupeng Yuan** received his Ph.D. degree in control theory and control engineering from Chongqing University, China, in 2016. Currently he is a senior engineer in CETC Chips Technology Group Co., LTD, Chongqing, China. His research activities are focused on research and development in intelligent sensor and Micro-Electro-Mechanical Systems applied to gas detection, photoelectric transmission and inertial navigation. He has published more than 30 peer reviewed papers.



**Zhijian Shang** is now pursuing a Ph.D. degree in atomic and molecular physics in the Institute of Laser Spectroscopy of Shanxi University, China. His research interests include optical sensors and photoacoustic spectroscopy.



**Xukun Yin** received his Ph.D. degree in atomic and molecular physics from Shanxi University, China, in 2020. From 2018–2019, he studied as a research associate in the electrical and computer engineering department, Rice University, Houston, USA. Currently he is an associate professor in the School of Optoelectronic Engineering of Xidian University. His research interests include optical sensors, laser spectroscopy techniques and insulation fault diagnosis of electrical equipment.



**Angelo Sampaolo** obtained his Master degree in Physics in 2013 and the PhD Degree in Physics in 2017 from University of Bari. He was an associate researcher in the Laser Science Group at Rice University from 2014 to 2016 and associate researcher at Shanxi University since 2018. Since May 2017, he was a Post-Doctoral Research associate at University of Bari and starting from December 2019, he is Assistant Professor at Polytechnic of Bari. His research activity has included the study of the thermal properties of heterostructured devices via Raman spectroscopy. Most recently, his research interest has focused on the development of innovative techniques in trace gas sensing, based on Quartz-Enhanced Photoacoustic Spectroscopy and covering the full spectral range from near-IR to THz. His achieved results have been acknowledged by a cover paper in *Applied Physics Letter* of the July 2013 issue.



2013 issue.

**Pietro Patimisco** obtained the Master degree in Physics (cum laude) in 2009 and the PhD Degree in Physics in 2013 from the University of Bari. Since 2018, he is Assistant professor at the Technical University of Bari. He was a visiting scientist in the Laser Science Group at Rice University in 2013 and 2014. Dr. Patimisco's scientific activity addressed both micro-probe optical characterization of semiconductor optoelectronic devices and optoacoustic gas sensors. Recently, his research activities included the study and applications of trace-gas sensors, such as quartz-enhanced photoacoustic spectroscopy and cavity enhanced absorption spectroscopy in the mid infrared and terahertz spectral region, leading to several publications, including a cover paper in *Applied Physics Letter* of the July



than 50 invited presentations at international conferences and workshops.

**Vincenzo Spagnolo** obtained the PhD in physics in 1994 from University of Bari. From 1997–1999, he was researcher of the National Institute of the Physics of Matter. Since 2004, he works at the Technical University of Bari, formerly as assistant and associate professor and, starting from 2018, as full Professor of Physics. Since 2019, he is vice-rector of the Technical University of Bari, deputy to technology transfer. He is the director of the joint-research lab PolySense between Technical University of Bari and THORLABS GmbH, fellow member of SPIE and senior member of OSA. His research interests include optoacoustic gas sensing and spectroscopic techniques for real-time monitoring. His research activity is documented by more than 220 publications and two filed patents. He has given more



**Lei Dong** received his Ph.D. degree in optics from Shanxi University, China, in 2007. From June, 2008 to December, 2011, he worked as a post-doctoral fellow in the Electrical and Computer Engineering Department and Rice Quantum Institute, Rice University, Houston, USA. Currently he is a professor in the Institute of Laser Spectroscopy of Shanxi University. His research activities are focused on research and development in laser spectroscopy, in particular photoacoustic spectroscopy applied to sensitive, selective and real-time trace gas detection, and laser applications in environmental monitoring, chemical analysis, industrial process control, and medical diagnostics. He has published more than 100 peer reviewed papers with > 2200 positive citations.



**Hongpeng Wu** received his Ph.D. degree in atomic and molecular physics from Shanxi University, China, in 2017. From 2015–2016, he studied as a joint Ph.D. student in the electrical and computer engineering department and rice quantum institute, Rice University, Houston, USA. Currently he is a professor in the Institute of Laser Spectroscopy of Shanxi University. His research interests include optical sensors and laser spectroscopy techniques.